ADVANCES IN ATMOSPHERIC SCIENCES, VOL. 31, JULY 2014, 779–786

Predictability of Winter Rainfall in South China as Demonstrated by the Coupled Models of ENSEMBLES

Se-Hwan YANG[1,2], LI Chaofan[3], and LU Riyu*[1]

[1]*State Key Laboratory of Numerical Modelling for Atmospheric Sciences and Geophysical Fluid Dynamics, Institute of Atmospheric Physics, Chinese Academy of Sciences, Beijing* 100029

[2]*University of the Chinese Academy of Sciences, Beijing* 100049

[3]*Center for Monsoon System Research, Institute of Atmospheric Physics, Chinese Academy of Sciences, Beijing* 100029

(Received 11 September 2013; revised 29 November 2013; accepted 6 December 2013)

ABSTRACT

Winter rainfall over South China shows strong interannual variability, which accounts for about half of the total winter rainfall over South China. This study investigated the predictability of winter (December–January–February; DJF) rainfall over South China using the retrospective forecasts of five state-of-the-art coupled models included in the ENSEMBLES project for the period 1961–2006. It was found that the ENSEMBLES models predicted the interannual variation of rainfall over South China well, with the correlation coefficient between the observed/station-averaged rainfall and predicted/area-averaged rainfall being 0.46. In particular, above-normal South China rainfall was better predicted, and the correlation coefficient between the predicted and observed anomalies was 0.64 for these wetter winters. In addition, the models captured well the main features of SST and atmospheric circulation anomalies related to South China rainfall variation in the observation. It was further found that South China rainfall, when predicted according to predicted DJF Niño3.4 index and the ENSO–South China rainfall relationship, shows a prediction skill almost as high as that directly predicted, indicating that ENSO is the source for the predictability of South China rainfall.

Key words: predictability, South China, winter rainfall, ENSO, ENSEMBLES

Citation: Yang, S.-H., C. F. Li, and R. Y. Lu, 2014: Predictability of winter rainfall in South China as demonstrated by the coupled models of ENSEMBLES. *Adv. Atmos. Sci.*, **31**(4), 779–786, doi: 10.1007/s00376-013-3172-2.

1. Introduction

Winter rainfall over South China displays large interannual variability relative to its total amount. The rainfall over South China ranges from 100 to 260 mm month^{-1}, while its interannual variations can even reach 50–130 mm month^{-1}, about half of the total winter rainfall (Li and Ma, 2012) The first leading mode of winter precipitation over China mainly reflects the South China rainfall variability (Wang and Feng, 2011), confirming the strong interannual variability in South China rainfall during winter. Therefore, more attention should be paid to the interannual variation and seasonal predictability of South China winter rainfall.

The El Niño–Southern Oscillation (ENSO) exerts significant impacts on South China winter rainfall (Tao and Zhang, 1998; Zhang and Sumi, 2002; Wang and Feng, 2011; Li and Ma, 2012). El Niño events result in more rainfall over South China in winter. During the winters of El Niño events, there is an anomalous anticyclone over the western North Pacific, and thus the anomalous lower-tropospheric southwesterly winds at the northwest flank of the anticyclonic anomaly transport more moisture to South China (Zhou et al., 2010; Li and Ma, 2012). Therefore, the anomalous anticyclone over the western North Pacific plays a key role in establishing the relationship between ENSO and South China winter rainfall. The main leading mode of winter rainfall over China, which appears mainly over South China, is also closely related to ENSO (Wang and Feng, 2011). This close relationship to ENSO could help with better prediction of winter rainfall over South China.

Apart from ENSO, the winter rainfall variability in South China is also affected by some other factors. Zhou (2011) pointed out that there is a significant correlation between the East Asian winter monsoon and South China rainfall. A strong East Asian winter monsoon can suppress the moisture transported by the southwesterly anomalies in the lower troposphere over South China and show impacts independent of ENSO on South China rainfall. Interannual variation of the East Asian winter monsoon is greatly related to anoma-

* Corresponding author: LU Riyu
Email: lr@mail.iap.ac.cn

lous mid-latitude atmospheric circulation (Chen et al., 2005). In addition, the second leading mode of winter rainfall over China, which also shows significant rainfall anomalies over South China, is also related to circulation anomalies over the mid-high latitudes (Wang and Feng, 2011).

Since the circulation anomalies in the middle and high latitudes have a low seasonal predictability, the predictability of South China winter rainfall may be greatly affected by these "noises". On the other hand, the close relationship with ENSO may make South China rainfall relatively highly predictable. However, the predictability of South China winter rainfall has not been documented in the literature. By using the hindcast results of current coupled models, this study investigated the prediction skills of South China winter rainfall and the contribution of ENSO to the predictability. Five state-of-the-art coupled models from ENSEMBLES, which was an EU-funded integrated project aimed at the development of an ensemble prediction system for seasonal prediction (van der Linden and Mitchell, 2009) were used in this study.

The remainder of the paper is organized as follows. In section 2 we describe the hindcasts and observational datasets used in the study. In section 3 we examine the predictability of interannual variability in South China winter rainfall and the associated circulation anomalies. Section 4 describes the contributions of ENSO to the predictability of winter rainfall over South China. And finally, section 5 provides a summary of the results.

2. Hindcasts and observational datasets

The ENSEMBLES models used in this study included those of the UK Met Office (UKMO), Météo-France (MF), the European Centre for Medium-Range Weather Forecasts (ECMWF), the Leibniz Institute of Marine Sciences at Kiel University (IFM-GEOMAR), and the Euro-Mediterranean Centre for Climate Change (CMCC-INGV). The ENSEMBLES project was a seasonal-to-annual multi-model project of the European Union aimed at developing a fully coupled atmosphere-ocean-land prediction systems (van der Linden and Mitchell, 2009). The models included major radiative forcing, no flux adjustments, and were initialized by using realistic estimates of the observed states. Nine initial conditions were run in each model. Table 1 shows a brief summary of the main model components with their resolutions. Readers are referred to Doblas-Relyes et al. (2009, 2010) and van der Linden and Mitchell (2009) for further details about the ENSEMBLES multi-model project and models.

The retrospective forecasts of all the models were performed for the period 1961–2006. The seasonal forecasts were initialized on the 1st of November and run for 14 months. The results for the subsequent DJF (December–January–February) are analyzed in this paper. The winter of one particular year is defined as the months from December of the previous year to February of the present year. For simplicity, only the multi-model ensemble (MME) prediction, which was calculated through simple composite analysis by applying equal weights to all models, is shown in this paper.

The observed datasets used for model verification included monthly mean National Centers for Environmental Prediction/National Center for Atmospheric Research (NCEP/NCAR) reanalysis data (Kalnay et al., 1996) and NOAA Extended Reconstructed SST V3 datasets for the period 1961–2006. The observed monthly precipitation datasets included those from the Global Precipitation Climatology Project (GPCP) for the period 1980–2006 (Adler et al., 2003) and the China Meteorological Administration (CMA) for the period 1961–2006, based on data from 160 stations.

3. Assessment of the prediction of South China winter rainfall

Figure 1 shows the standard deviations (SDs) of winter (DJF) rainfall over China for the period 1961–2006. As can be seen, the interannual variability of winter rainfall was considerably large over South China. The corresponding SDs were around 30 mm month^{-1} and were significantly larger than other regions of China. We selected 33 stations where the SDs were larger than 20 mm month^{-1}, and the South

Table 1. Description of the five models used in this study.

	AGCM		OGCM	
Partner	Model	Resolution	Model	Resolution
ECMWF	IFS-CY31R1	T159/L62	HOPE	0.3°–1.4°/L29
IFM-GEOMAR	ECHAM5	T63/L31	MPI-OM1	1.5°/L40
MF	APPEGE4.6	T63	OPA8.2	2°/L31
UKMO	HadGEM2-A	N96/L38	HadGEM2-O	0.33°–1°/L20
CMCC-INGV	ECHAM5	T63/L19	OPA8.2	2°/L31

IFS-CY31R1: Integrated Forecast System CY31R1;
HOPE: Hamburg Ocean Primitive Equation Model;
ECHAM5: European Community–Hamburg model (version 5);
MPI-OM1: Max Planck Institute Ocean Model (version 1);
APPEGE4.6: Action de Recherche Petite Echelle Grande Echelle (version 4.6);
OPA8.2: Océan Parallélisé (version 8.2);
HadGEM2-A: Hadley Centre Global Environmental Model (version2–Atmosphere);
HadGEM2-O: HadGEM (version2–Ocean).

China rainfall was defined by rainfall averaged over these 33 stations.

Figure 2 shows normalized DJF-mean South China precipitation anomalies during the period 1961–2006. In order to compare with observations, the predicted South China rainfall was calculated as the average rainfall over the land region (23°–30°N, 110°–120°E), which covers the majority of the stations with larger interannual variability. Figure 2 indicates that the interannual variation of South China rainfall was well captured by the model prediction. The correlation coefficient between the observation and MME result was 0.46, reaching the 99.8% statistical confidence level. This good prediction was also reflected by comparing year-by-year between the model prediction and observations. Furthermore, the models predicted the South China rainfall anomalies well during most of the wetter years. For instance, the positive South China rainfall anomalies in 1983 and 1998, which correspond to strong El Niño cases, were predicted rather well by the models. The correlation coefficient between the predicted and observed anomalies was 0.64 for the wetter winters, i.e., winters with an observed positive rainfall anomaly, and this correlation coefficient was much higher than that for dry winters (0.19). The correlation coefficient was calculated by the following formula:

$$r = \frac{\sum_{i}^{n} X_{\mathrm{m}}(i) X_{\mathrm{o}}(i)}{\sqrt{\sum_{i}^{n} X_{\mathrm{m}}(i)^2} \sqrt{\sum_{i}^{n} X_{\mathrm{o}}(i)^2}},$$

where n is the number of wetter (dry) years, and $X_{\mathrm{m}}(i)$ and $X_{\mathrm{o}}(i)$ are the predicted and observed anomalies for the ith wetter (dry) year, respectively.

The above result is consistent with previous observational studies (Zhang et al., 1996, 1999; Chen, 2002), which indicated that there are significantly positive rainfall anomalies in South China during El Niño winters, but much weaker and negative rainfall anomalies during La Niña winters. In addition, the South China rainfall showed a clear asymmetry between positive and negative anomalies in the observation. This asymmetry can also be illustrated by the intensity of positive and negative rainfall anomalies. Positive rainfall anomalies tended to be stronger and appear in fewer years (17 years), but negative anomalies were relatively weaker but appeared in more years (29 years). This asymmetry can be further illustrated by the skewness, which can be used as a measure of the extent to which a probability distribution of a variable is concentrated on one side of the mean. The skewness of South China rainfall anomalies was 0.76 in the observation. The MME predictions captured this observed feature, showing a skewness of 0.53.

Figure 2 also shows that South China winter rainfall had an increasing trend, with an amplitude of 0.18 mm (10 yr)$^{-1}$. The model predictions captured this increasing trend, but showed a weaker amplitude [0.10 mm (10 yr)$^{-1}$], about half that of the observed one. This result implies that the increasing trend of South China winter rainfall may be partially due to atmosphere–ocean interactions.

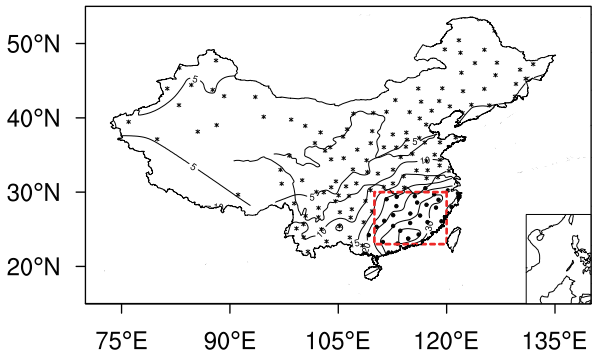

Fig. 1. SDs of winter rainfall (mm month^{-1}) in China during the period 1961–2006 (solid line). The asterisks and dots denote the locations of the 160 stations in China with SDs lower and larger than 20 mm month^{-1}, respectively. The box denotes the region used to define South China in the model.

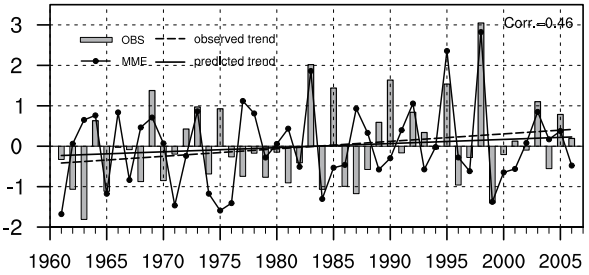

Fig. 2. Normalized DJF South China precipitation anomalies in the observation (bars) and prediction (line), and the long-term trend in the observation (dashed straight line) and prediction (solid straight line). The top right value is the correlation coefficient between the observation and prediction.

Figure 3 shows the spatial distribution of temporal correlation coefficients (TCCs) between the observed and predicted rainfall for the period 1980–2006. A high TCC indicates that there is a close relationship between the forecast and observation, and thus a high predictability. In general, high TCCs were mainly located in the tropical area. The winter rainfall around the Philippine Sea was predicted very well with TCCs higher than 0.8. In addition, the TCCs were also high over the region extending from South China to the subtropical western North Pacific. The TCCs were around 0.6 in South China, confirming that South China winter rainfall is highly predictable. These TCCs were relatively higher than the correlation coefficient (0.46) between the observed and predicted rainfall anomalies averaged over South China for the period 1961–2006. This difference mainly resulted from the difference in the analysis periods. The correlation coefficient between the observed/station-averaged and predicted/area-averaged South China rainfall anomalies was 0.64 during 1980–2006, greater than that (0.46) during 1961–2006, and much greater than that (0.05) during 1961–79. This result suggests that the predictability of South China rainfall exhibits a decadal change, which may be related to the decadal change in the ENSO–South China rainfall relation-

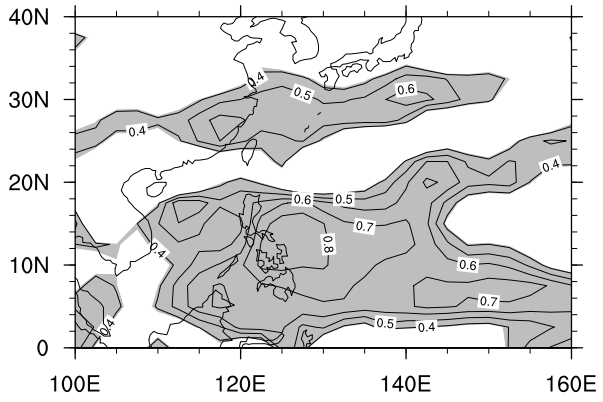

Fig. 3. TCCs of winter precipitation between the observation and prediction for the period 1980–2006. Shading indicates the regions where anomalies are statistically significant at the 95% confidence level.

ship (Li and Ma, 2012).

Figure 4 shows the SST, 200 and 850-hPa wind anomalies regressed onto South China rainfall in the observation and MME prediction. In the observation, the spatial distribution of SST anomalies exhibited a typical El Niño-like pattern: there were significant positive correlations in the tropical central and eastern Pacific and the tropical Indian Ocean, and a significant negative correlation over the western North Pacific (Fig. 4a). It suggests that ENSO is closely related to the interannual variation of South China winter rainfall, which is consistent with previous studies (Tao and Zhang, 1998; Zhang and Sumi, 2002; Wang and Feng, 2011). In the upper troposphere, there was an anomalous cyclone over South China and the subtropical western North Pacific (Fig. 4c). Associated with this anomalous cyclone, significant westerlies were found over India, the Bay of Bengal, Indo-China Peninsula, and the Maritime Continent. There was an anomalous anticyclone north of this anomalous cyclone. On the contrary, in the lower troposphere, anomalous southwesterlies appeared

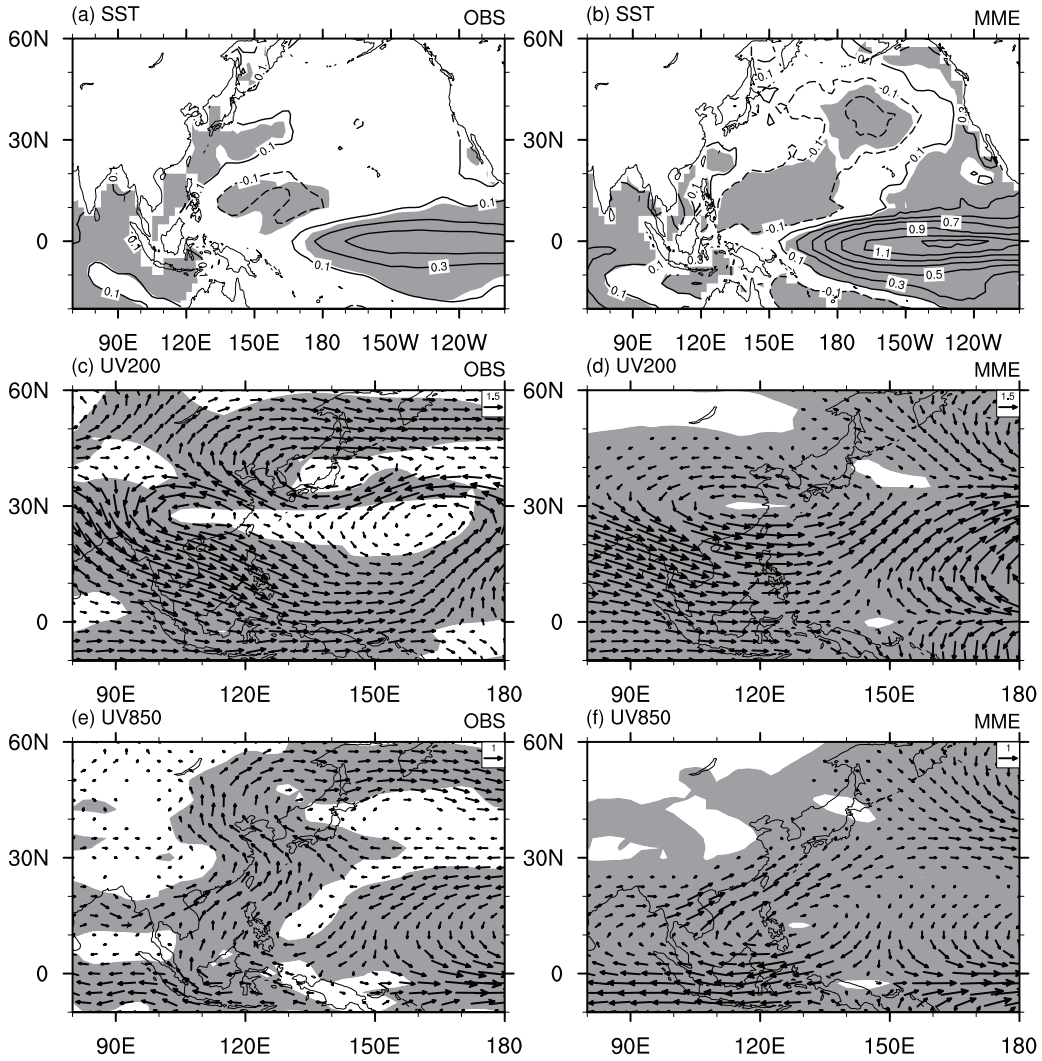

Fig. 4. Regression of SST anomalies (°C, top), wind anomalies (m s^{-1}) at 200 (middle) and 850 hPa (bottom) onto South China winter precipitation in the observation (left) and prediction (right) for the period 1961–2006. Shading indicates the regions where anomalies are statistically significant at the 95% confidence level.

over South China (Fig. 4e). These anomalies were connected to the anomalous anticyclone over the tropical western North Pacific, and induced more moisture transport to South China and more rainfall over South China (Wu et al., 2003; Zhou et al., 2010; Li and Ma, 2012). The anomalous southwesterlies turned to southeasterly and southerly anomalies in East Asia and Northeast Asia, associated with the anomalous anticyclone over East Asia and the mid-latitude western North Pacific. These upper- and lower-tropospheric wind anomalies are consistent with previous results (Zhou and Wu, 2010; Zhou, 2011; Li and Ma, 2012).

The ENSEMBLES prediction captured most of the features of anomalies associated with the South China rainfall variability well (Figs. 4b, d and f). The El Niño-like SST anomalies were well captured by the models (Fig. 4b). However, the SST anomalies in the tropical central and eastern Pacific were greater in the prediction than those in the observation. The Niño3.4 index corresponding to one SD of South China rainfall was 0.88°C in the prediction, and was much greater than that (0.52°C) in the observation. This implies that the relationship between ENSO and South China rainfall variability was overestimated in the prediction, which is expected since "noises" were suppressed and "signals" were highlighted in the MME results. The ENSO–South China rainfall relationship is further examined in the following section. In addition, the wind anomalies related to South China rainfall were also well captured by the models (Figs. 4d, f). The models captured the anomalous cyclone over South China and the western Pacific in the upper troposphere. They also captured the southwesterlies over the coastal area of South China in the lower troposphere. These upper- and lower-tropospheric wind anomalies play a crucial role in inducing more rainfall in South China during winter (Zhou, 2011). However, it should be mentioned that the well-captured wind anomalies related to South China rainfall were mainly concentrated over the tropical and subtropical regions. There were appreciable discrepancies in the mid-latitude wind anomalies between the MME prediction and observations. The anomalous upper-tropospheric anticyclone anomaly and lower-tropospheric southerly anomaly over Northeast Asia, which appeared in the observation, were not apparent, or were much weakened, in the prediction.

Figure 5 shows the spatial distribution of the TCCs for SST, 200 and 850-hPa winds between the prediction and observation. It reveals that most of the SST and circulation anomalies related to South China rainfall are highly predictable. High TCCs for SST anomalies appeared over the tropical Pacific and Indian Ocean (Fig. 5a). Good prediction of 200-hPa zonal wind appeared over the tropical region west of 140°E and mid-latitude region along 35°N (Fig. 5b). These high TCCs corresponded well with the westerly anomaly over the tropical region and the easterly anomaly along 35°N, which were associated with the anomalous cyclone in the upper troposphere (Fig. 4c). In addition, both zonal and meridional wind anomalies were highly predictable over the coastal area of South China in the lower troposphere: the TCCs were around 0.7 and 0.5 for zonal and meridional wind anomalies, respectively (Figs. 5c, d). Therefore, the southwesterly (or northeasterly) anomalies associated with South China rainfall have a high predictability. However, the TCCs for circulation anomalies were very weak over the regions with latitudes higher than 40°N, suggesting a weak capability of the models in predicting the mid-latitude anomalous circulation related to South China rainfall.

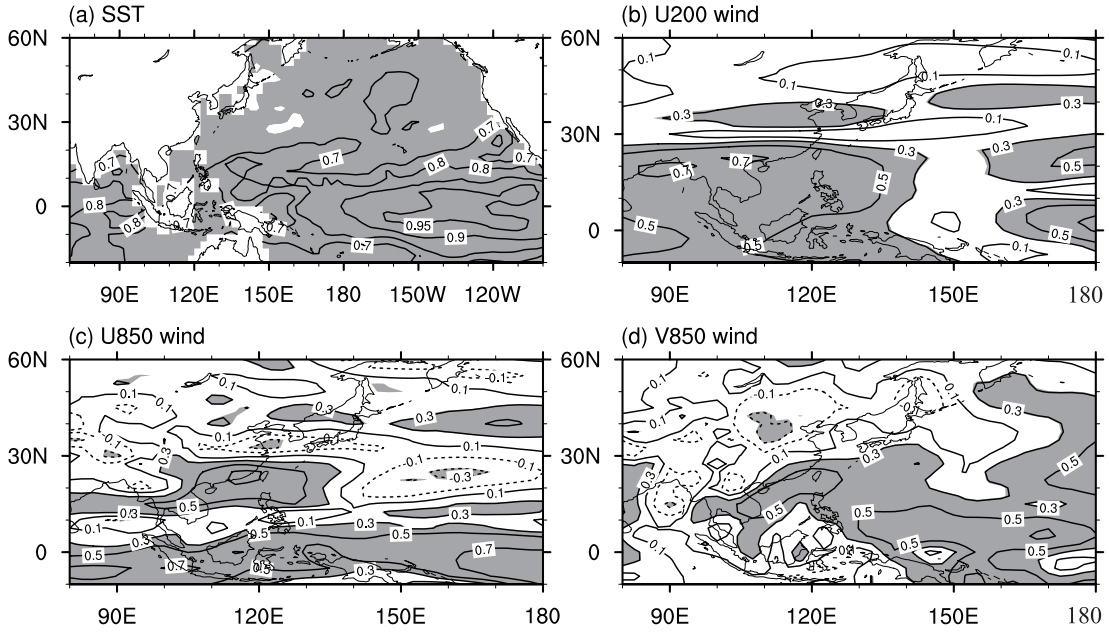

Fig. 5. TCCs for (a) SST, (b) zonal winds at 200 hPa, (c) zonal winds and (d) meridional winds at 850 hPa between the observation and prediction during the period 1961–2006. Shading indicates the regions where anomalies are statistically significant at the 95% confidence level.

4. Predictability of South China winter rainfall related to ENSO

Figure 6 shows the distribution of correlation coefficients between winter precipitation and Niño3.4 index for 27 years (1980–2006). It reveals that ENSO has a close relationship with South China rainfall, indicated by the positive correlations over South China, which showed a band-like distribution extending from South China to the subtropical western North Pacific. In addition, there were significant negative correlations around the Philippines over the tropical region. These regions of significant positive or negative correlations corresponded well to those of high TCCs of winter precipitation (Fig. 3). The correlation coefficient between the South China rainfall index (shown in Fig. 2) and Niño3.4 index was 0.51 in the observation during the period 1961–2006, exceeding the 99.9% statistical confidence level, which is consistent with previous studies (e.g., Zhou and Wu, 2010; Li and Ma, 2012). On the contrary, the correlation coefficient between these two indexes was 0.83 in the MME prediction. This suggests that the model prediction overestimated the relationship between ENSO and South China rainfall, which is consistent with the result shown in Fig. 4b. In addition, interannual variation of the SSTs in the equatorial central and eastern Pacific was highly predictable (Fig. 5a). The correlation coefficient between the predicted and observed Niño3.4 index was 0.97. These results imply that model prediction of South China rainfall relies greatly on ENSO predictability, and the Niño3.4 index can be used as a predictor for South China winter rainfall.

The cross-validated forecast was used to further investigate the contributions of ENSO to the prediction skill of South China rainfall. Cross-validated forecasts, which in this case considered 45 years as the training period and the rainfall anomaly in the target year for downscaling, can avoid the over-fitting in the downscaling scheme and have been used in many previous studies (e.g., Feddersen et al., 1999; Kang et al., 2004; Yun et al., 2005; Zhu et al., 2008). Using the DJF Niño3.4 index as a predictor, the regressed coefficient was obtained from the observed Niño3.4 index and South China rainfall in the 45 training years. Then, the cross-validated South China rainfall was regressed onto the predicted Niño3.4 index of the MME prediction in the target year. This method can be described simply as predicting the DJF Niño3.4 index first, and then predicting South China rainfall by using the Niño3.4 index as a predictor.

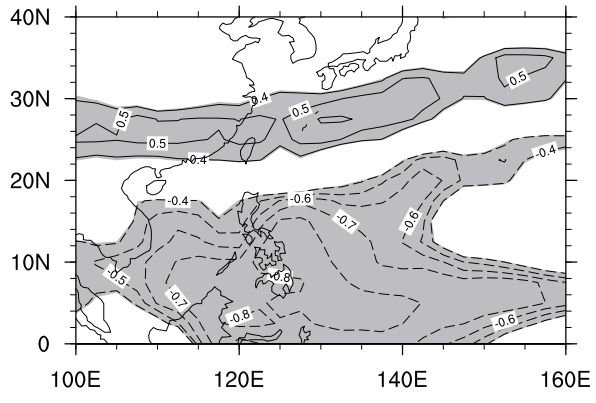

Fig. 6. Correlation coefficients between winter precipitation and the Niño3.4 index for the period 1980–2006 in the observation. Shading indicates the regions where anomalies are statistically significant at the 95% confidence level.

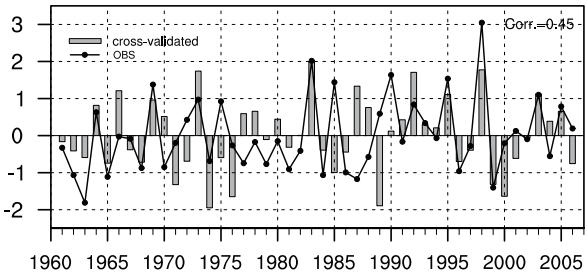

Fig. 7. The same as Fig. 2, but for South China winter rainfall anomalies statistically deduced by predicted Niño3.4 index.

Figure 7 illustrates the normalized series of South China rainfall anomalies predicted through the above-mentioned approach. For convenience, this time series is simply referred to as "ENSO-predicted" in the following analysis. The correlation coefficient between the ENSO-predicted and observed South China rainfall reached 0.45. This correlation coefficient was considerably close to that of the coupled models of ENSEMBLES (0.46, shown in Fig. 2). The ENSO-predicted and directly predicted South China rainfall also had a high correlation coefficient (0.79). This reveals that ENSO is the main source for the good prediction skill of the coupled models for South China rainfall variation. Furthermore, when the observed Niño3.4 index in November of the previous year was used as the predictor based on the cross-validated regression, the correlation coefficient between the predicted and observed South China rainfall index reached 0.40. This further suggests that the intimate relationship between ENSO and South China rainfall plays a critical role in the good prediction skill of South China rainfall in the current coupled models, and the ENSO predictions by the models are better than the persistency.

Figure 8 shows the regression of SST and winds at 200 and 850 hPa onto Niño3.4 index in the observation and MME prediction. The main features of ENSO-related anomalies, including the SST pattern, the cyclone in the upper troposphere and the southwesterlies in the lower troposphere, showed great similarity to those related to South China rainfall (Fig. 4). This similarity confirms that ENSO results in the main anomalies that influence the interannual variation of South China rainfall. In addition, Fig. 8 also indicates that the observed ENSO-related anomalies were well captured. The spatial distribution and intensity of the SST and circulation anomalies were quite similar to those in the observation. This similarity suggests that the coupled models describe the relationship between ENSO and South China rainfall well.

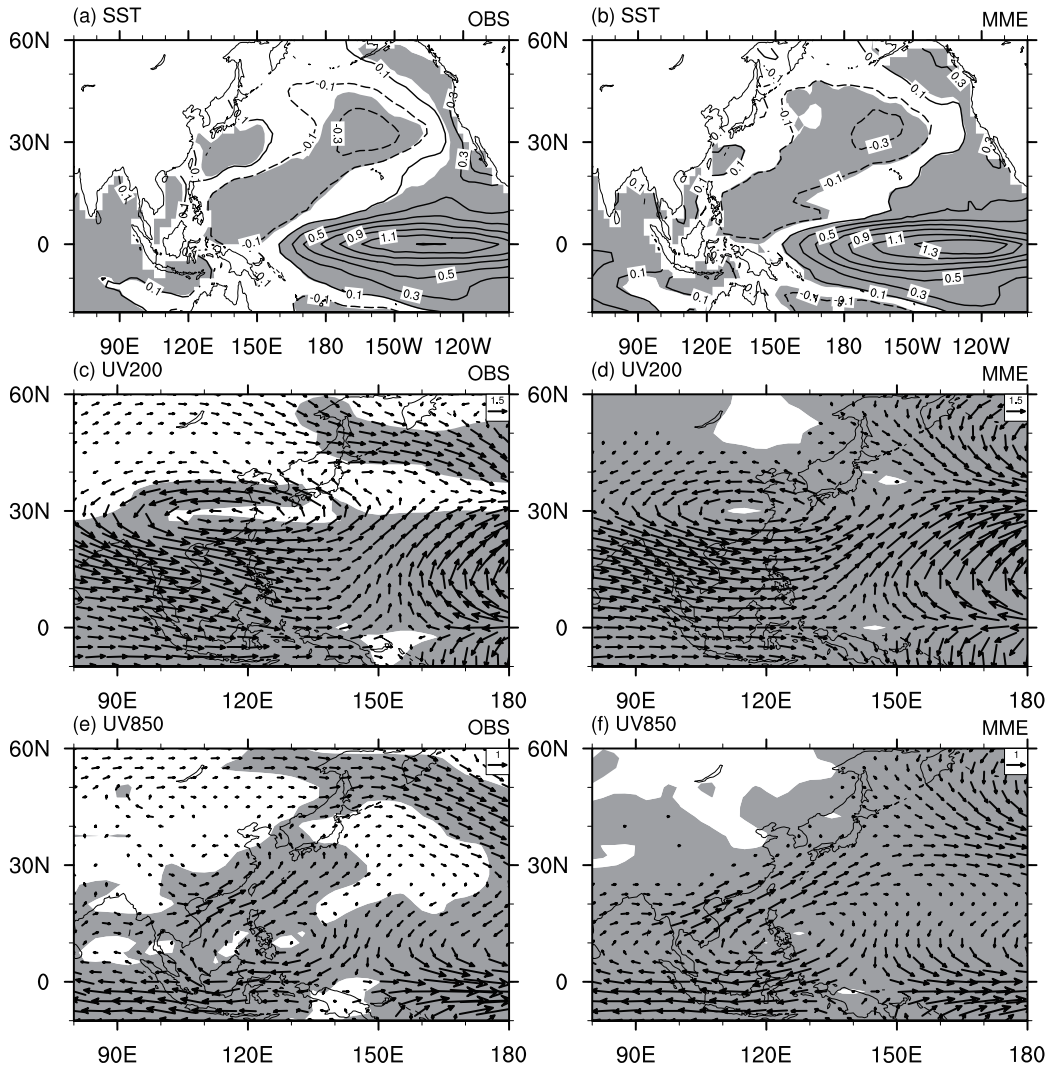

Fig. 8. The same as Fig. 4, but regressed onto the Niño3.4 index.

5. Summary

This study investigated the seasonal predictability of winter rainfall in South China. The retrospective forecasts of five atmosphere–ocean coupled models from a multi-model project named ENSEMBLES during the period 1961–2006 were analyzed.

The interannual variability of winter rainfall over South China exhibited a high predictability. The correlation coefficient between the predicted and observed rainfall anomalies averaged over South China was 0.46, reaching the 99.8% statistical confidence level. In addition, the good prediction of South China rainfall was reconfirmed by the high predictability of the associated SST and atmospheric circulation anomalies, characterized by an ENSO-like SST pattern, anomalous cyclone/anticyclone over South China in the upper troposphere, and anomalous southwesterlies/northeasterlies in the lower troposphere. Furthermore, the models successfully captured the relationship of South China rainfall with these SST and wind anomalies.

In addition, the models better predicted the South China rainfall anomalies when the anomalies were positive. The correlation coefficient between the predicted and observed anomalies was 0.64 for winters of positive rainfall anomalies in the observation during the period 1961–2006, much higher than that (0.19) for winters of negative rainfall anomalies. This result can be explained by the asymmetry in the relationship between ENSO and South China rainfall: South China rainfall anomalies are significantly and strongly positive during El Niño winters but very weak during La Niña winters in observations (Zhang et al., 1996, 1999; Chen, 2002). This asymmetry in the relationship between ENSO and South China rainfall induced a positive skewness (0.76) of South China rainfall in the observation, and the MME predictions captured this observed feature, showing a skewness of 0.53.

It was found that the good prediction skill of South China rainfall can be attributed to the close relationship between ENSO and South China rainfall. A cross-validated forecast was used to demonstrate the influence of ENSO on the pre-

diction skill of South China rainfall. The correlation coefficient between observed South China rainfall anomalies and the cross-validation regressed onto the Niño3.4 index in winter was 0.45. This correlation coefficient was almost identical to the prediction skill (0.46) directly shown by the models. Thus, it can be concluded that ENSO is the source of South China rainfall predictability at the interannual scale.

Acknowledgements. We thank the anonymous reviewers for their comments and suggestions, which greatly helped us to improve the presentation of this paper. This work was supported by the National Natural Science Foundation of China (Grant Nos. 41305067 and 41320104007).

REFERENCES

Adler, R. F., and Coauthors, 2003: The Version-2 Global Precipitation Climatology Project (GPCP) monthly precipitation analysis (1979–Present). *Journal of Hydrometeorology*, **4**, 1147–1167.

Chen, W., 2002: Impacts of El Niño and La Niña on the cycle of the East Asian winter and summer monsoon. *Chinese J. Atmos. Sci*., **26**, 595–610. (in Chinese)

Chen, W., S. Yang, and R.-H. Huang, 2005: Relationship between stationary planetary wave activity and the East Asian winter monsoon. *J. Geophys. Res.*, **110**, D14110, doi: 10.1029/2004JD005669.

Doblas-Reyes, F. J., and Coauthors, 2009: Addressing model uncertainty in seasonal and annual dynamical ensemble forecasts. *Quart. J. Roy. Meteor. Soc.*, **135**, 1538–1559.

Doblas-Reyes, F. J., A. Weisheimer, T. N. Palmer, J. M. Murphy, and D. Smith, 2010: Forecast quality assessment of the ENSEMBLES seasonal-to-decadal Stream 2 hindcasts. ECMWF/TM-No. 621, 45 pp.

Feddersen, H., A. Navarra, and M. N. Ward, 1999: Reduction of model systematic error by statistical correction for dynamical seasonal prediction. *J. Climate*, **12**, 1974–1989.

Kalnay, E., and Coauthors, 1996: The NCEP/NCAR 40 year reanalysis project. *Bull. Amer. Meteor. Soc.*, **77**, 437–471.

Kang, I.-S., J.-Y. Lee, and C.-K. Park, 2004: Potential predictability of a dynamical seasonal prediction system with systematic error correction. *J. Climate*, **17**, 834–844.

Li, C., and H. Ma, 2012: Relationship between ENSO and winter rainfall over Southeast China and its decadal variability. *Adv. Atmos. Sci.*, **29**, 1129–1141, doi: 10.1007/s00376-012-1248-z.

Tao, S. Y., and Q. Zhang, 1998: Response of the Asian winter and summer monsoon to ENSO events. *Scientia Atmospherica Sinica*, **22**, 399–407. (in Chinese)

van der Linden, P., and F. J. B. Mitchell, Eds., 2009: ENSEMBLES: Climate change and its impact: Summary of research and results from ENSEMBLES project. Met Office Hadley Centre, FitzRoy Road, Exeter EX1 3PB, UK, 160 pp.

Wang, L., and J. Feng, 2011: Two major modes of the wintertime precipitation over China. *Chinese J. Atmos. Sci*., **35**, 1105–1116. (in Chinese)

Wu, R. G., Z. Z. Hu, and B. P. Kirtman, 2003: Evolution of ENSO-related rainfall anomalies in East Asia. *J. Climate*, **16**, 3742–3758.

Yun, W. T., L. Stefanova, A. K. Mitra, T. S. V. Vijaya Kumar, W. Dewar, and T. N. Krishnamurti, 2005: A multi-model superensemble algorithm for seasonal climate prediction using DEMETER forecast. *Tellus*, **57**, 280–289.

Zhang, R. H., and A. Sumi, 2002: Moisture circulation over East Asia during El Niño episode in northern winter, spring and autumn. *J. Meteor. Soc. Japan*, **80**, 213–227.

Zhang, R. H., A. Sumi, and M. Kimoto, 1996: Impact of El Niño on the East Asian monsoon: A diagnostic study of the '86/87 and '91/92 events. *J. Meteor. Soc. Japan*, **74**, 49–62.

Zhang, R. H., A. Sumi, and M. Kimoto, 1999: A diagnostic study of the impact of El Niño on the precipitation in China. *Adv. Atmos. Sci.*, **16**, 229–241.

Zhou, L.-T., 2011: Impact of East Asian winter monsoon on rainfall over southeastern China and its dynamical process. *Int. J. Climatol.*, **31**, 677–686.

Zhou, L.-T., and R. G. Wu, 2010: Respective impacts of the East Asian winter monsoon and ENSO on winter rainfall in China. *J. Geophys. Res.*, **115**, D02107, doi: 10.1029/2009JD012502.

Zhou, L.-T., C.-Y. Tam, W. Zhou, and J. C. L. Chan, 2010: Influence of South China Sea SST and the ENSO on winter rainfall over South China. *Adv. Atmos. Sci.*, **27**, 832–844, doi: 10.1007/s00376-009-9102-7.

Zhu, C. W., C.-K. Park, W.-S. Lee, and W.-T. Yun, 2008: Statistical downscaling for multi-model ensemble prediction of summer monsoon rainfall in the Asia-Pacific region using geopotential height field. *Adv. Atmos. Sci.*, **25**, 867–884, doi: 10.1007/s00376-008-0867-x.